

# We are IntechOpen, the world's leading publisher of Open Access books Built by scientists, for scientists

6,900

Open access books available

186,000

International authors and editors

200M

Downloads

Our authors are among the

154

Countries delivered to

TOP 1%

most cited scientists

12.2%

Contributors from top 500 universities



WEB OF SCIENCE™

Selection of our books indexed in the Book Citation Index  
in Web of Science™ Core Collection (BKCI)

Interested in publishing with us?  
Contact [book.department@intechopen.com](mailto:book.department@intechopen.com)

Numbers displayed above are based on latest data collected.  
For more information visit [www.intechopen.com](http://www.intechopen.com)



# Ultrasonic and Spectroscopic Techniques for the Measurement of the Elastic Properties of Nanoscale Materials

Marco G. Beghi

## Abstract

Materials at the nanoscale often have properties which differ from those they have in the bulk form. These properties significantly depend on the production process, and their measurement is not trivial. The elastic properties characterize the ability of materials to deform in a reversible way; they are of interest by themselves, and as indicators of the type of nanostructure. As for larger scale samples, the measurement of the elastic properties is more straightforward, and generally more precise, when it is performed by a deformation process which involves exclusively reversible strains. Vibrational and ultrasonic processes fulfill this requirement. Several measurement techniques have been developed, based on these processes. Some of them are suitable for an extension towards nanometric scales. Until truly supramolecular scales are reached, the elastic continuum paradigm remains appropriate for the description and the analysis of ultrasonic regimes. Some techniques are based on the oscillations of purpose-built testing structures, mechanically actuated. Other techniques are based on optical excitation and/or detection of ultrasonic waves, and operate either in the time domain or in the frequency domain. A comparative overview is given of these various techniques.

**Keywords:** elasticity, vibrations, ultrasonics, surface waves, resonators, thin layers, nanorods

## 1. Introduction

Solid materials exist when the atoms find a configuration in which their potential energy has at least a local minimum, around which a stability region exists. Irrespective of the high number of degrees of freedom, and with rare exceptions, in the neighborhood of any minimum a more or less narrow interval exists, in which the potential energy is well represented by quadratic terms, higher order terms becoming negligible. A quadratic potential energy means an elastic restoring force, meaning that, when considering free motion around a stable equilibrium configuration, vibrational excitations are expected, which have a time periodicity. Periodicity can be represented by a frequency, or an angular frequency  $\omega$ , which is obviously determined by the properties of the physical system, namely in terms of stiffness and inertia. This general consideration applies from the atomic scale up to the full macroscopic scale, at which continuum models are appropriate.

When looking at the atomic motions, stiffness and inertia are given by the interatomic forces and the atomic masses. A distinction can be proposed among vibrational excitations, based on the phase difference between the motions of different atoms. Excitations exist in which when considering atoms at progressively decreasing distances, down to first neighbors, the phase difference between their displacements does not tend to zero. Examples are the vibrations of molecules, or the optical phonons in a crystalline structure. In this case the average displacement evaluated over a group of neighboring atoms does not have a relevant meaning, since the displacement of single atoms can be significantly different from the average one, and since the average can be null (as in the case of isolated molecules) or close to zero even in presence of atomic motions of significant amplitude. Excitations instead exist in which the phase difference between displacements of atoms located at smaller and smaller distances, down to nearest neighbors spacing, are smaller and smaller. Examples are the acoustic phonons in a crystalline structure. In this case the average displacement evaluated over a group of neighboring atoms becomes fully representative of the displacement of single atoms, and is the natural bridge towards a description of the continuum type, with a displacement vector field  $\mathbf{u}(\mathbf{r}, t) = u(x_1, x_2, x_3, t)$  which is a continuous function of the position vector  $\mathbf{r} = (x_1, x_2, x_3)$  and of time  $t$ . Excitations of this type are called acoustic excitations.

The description by the continuous vector field of displacement, and consequently by the tensor fields of strain and stress, is appropriate at scales which go from the supramolecular one, of the order of the nanometer or slightly more, at which the above-mentioned average begins to be meaningful, up to the fully macroscopic one. In the elastic continuum model [1–3] the potential energy is a quadratic function of strains, the coefficients of the expansion being the elements of the tensor of the elastic constants  $[C_{ijmn}]$ , conveniently represented in compact Voigt notation as  $[C_{kl}]$ . The stiffness being represented by these tensor elements, or by some functions of them which are specific elasticity moduli, and the inertia being represented by the mass density  $\rho$ , the equations of motion of the continuous medium are the elastodynamic equations. In the limit of an infinite homogeneous medium, which is symmetric to any translation in position and in time, the fundamental excitations are conveniently taken as waves, which, besides being periodic in time, are periodic in space, as described by a wavelength  $\lambda$  or a wave vector  $\mathbf{k}$ , with  $|\mathbf{k}| = 2\pi/\lambda$ . These fundamental solutions are characterized by dispersion relations  $\omega(\mathbf{k})$ , which are determined by the stiffness and the inertia properties [1–3].

It has been recognized, since long ago, that the measurement of the vibrational excitations gives access to these properties [4]. In particular, if the inertial properties (atomic masses or mass densities) are known, the stiffness properties can be measured. In both the atomic and the continuum case, they represent the curvature of the potential energy in the neighborhood of its minimum, and therefore they contain information, respectively, about the interatomic bonding and about the stiffness of solids, in its usual meaning. A whole wealth of experimental techniques has therefore been developed, which exploit vibrational excitations to measure material properties [4]. A general advantage of all the measurement techniques based on vibrational excitations is that they can exploit displacements of small amplitude, confined in the neighborhood of the equilibrium position, in which the representation of the potential energy by only the quadratic terms is an excellent approximation. In other words, higher order terms of the potential do not interfere, and, in the case of continua, non-elastic deformation mechanisms, other than the simple, reversible, stretching of interatomic bonds, are not activated.

Vibrational excitations of non-acoustic type, which cannot be described by a continuous field of displacements, are not treated by mechanics, but rather by solid

state physics, which measures them by techniques like Raman spectroscopy, to obtain various information at atomic level, including that concerning the interatomic forces. They are not considered here.

Vibrational excitations of the acoustic type, instead, have the same properties from the supramolecular, or nanometric, scale, up to the kilometeric scale and above. Accordingly, techniques based on acoustic excitations are exploited to measure the stiffness properties of objects of various sizes, up to dams, and are exploited for geological investigations. These methods measure the dynamic, or adiabatic, elastic moduli; these moduli do not coincide with the isothermal moduli which are measured in monotonic tests (if strain rate is not too high), but in elastic solids the difference between adiabatic and isothermal moduli seldom exceeds 1% [2].

At the other extreme of the size scale, some techniques can be pushed to measure microscopic objects, down to carbon nanotubes. Nanomechanics precisely addresses the behavior of microscopic objects; in this chapter we consider measurement techniques based on vibrational excitations of the acoustic type, which are pushed to measure small objects, towards the size at which the same concept of 'acoustic excitations' begins to lose significance, as well as that of the strain field. Techniques based on vibrational excitations, and in particular optical techniques, which avoid mechanical contact, are particularly prone to be applied to small objects, for which the contact with actuators or sensors becomes critical. In many cases, the mechanical properties of materials at this scale are of interest for the design and production of microsystems which operate dynamically; in these cases, the dynamic, adiabatic, moduli, are precisely those of interest.

The next section summarizes some basic concepts about free acoustic excitations in finite objects. The following two sections give an overview of several measurement techniques, which are grouped in two categories. First, those that exploit the oscillations of purpose-built testing structures, which are mechanically actuated, often by piezoelectric means. Secondly, the techniques which measure the properties of ultrasonic waves, that are typically excited and/or detected by optical means. These techniques can be further subdivided among those which operate in the time domain and those which operate in the frequency domain.

## 2. Acoustic excitations in confined media

Displacements and strains in the elastic continuum model in the absence of body forces, obey the elastodynamic equations; for homogeneous media they are [1–3]

$$\rho \frac{\partial^2 u_i}{\partial t^2} = \sum_{j,m,n} C_{ijmn} \frac{\partial^2 u_m}{\partial x_j \partial x_n}, i = 1, 2, 3.. \quad (1)$$

The invariance to any translation in time is the root of the harmonic time dependence of the fundamental solutions, characterized by the circular frequency  $\omega$ , which allows to transform the equations into the Helmholtz equations. The invariance to any translation in position, in practically infinite media, is the root of the harmonic space dependence of the fundamental solutions, which are traveling monochromatic harmonic waves, characterized by the wave vector  $\mathbf{k}$ . The dispersion relations  $\omega(\mathbf{k})$  are determined by the properties of the medium. The displacement vector  $\mathbf{u}$  having three independent components, the dispersion relation has three branches, which can be classified according to the relative orientations of the vectors  $\mathbf{u}$  and  $\mathbf{k}$ , i.e. according to their polarization: in an isotropic medium, one longitudinal and two transversal modes [1–3].



The elastic continuum model has no intrinsic length scales; as mentioned above it loses significance at the nanometric scale, while in an infinite medium, which also from the geometrical point of view has no intrinsic length scale, it does not have an upper limit of size. The wavelengths span in a continuous way this whole infinite interval, and the corresponding angular frequencies go, in continuity, from null frequencies for  $\lambda \rightarrow \infty$ , i.e.  $\mathbf{k} \rightarrow \mathbf{0}$ , up to a not sharply defined upper limit, corresponding to the shortest meaningful wavelengths. The absence of intrinsic length scales implies that all these wavelengths behave in exactly the same way, and the dispersion relations are simply linear:  $\omega = v|\mathbf{k}|$ , the velocities being independent from  $|\mathbf{k}|$ , i.e. these modes are non dispersive. In the general anisotropic medium the velocities depend on the direction of  $\mathbf{k}$ , while in the isotropic case they do not, and the velocities  $v_l$  and  $v_t$  of the longitudinal and transversal modes are respectively [1–3]

$$v_t = \sqrt{C_{44}/\rho} \text{ and } v_l = \sqrt{C_{11}/\rho}, \quad (2)$$

thermodynamic stability requiring that  $v_t < v_l$ .

Rupture of the unconditional translational symmetry by some kind of boundary condition, which introduces some kind of confinement, induces the appearance of further acoustic modes, namely standing waves. The consequences of confinement can be appreciated also without abandoning the relative simplicity of the isotropic model. They are already present, in a paradigmatic way, in the case which is probably the simplest rupture of the infinite translational symmetry: the plane external surface of a semi-infinite medium. The invariance to any translation in time is not altered, and correspondingly the acoustic modes remain periodic in time, associated to a circular frequency  $\omega$ . In the same way, the invariance of the medium to any translation in the plane of the surface is not modified, and correspondingly the acoustic modes remain periodic, and traveling, in this plane. This periodicity is conveniently represented by a wave vector  $\mathbf{k}_{\parallel}$  parallel to the surface, which identifies a direction and a repetition period. Considering media which possess in-plane isotropy, the direction of  $\mathbf{k}_{\parallel}$  becomes irrelevant and, in order to simplify the notation, we introduce here the symbol  $\lambda_{\parallel} \equiv 2\pi/|\mathbf{k}_{\parallel}|$ , which seems inappropriate because wavelength is not a vectorial quantity, but must be understood as a compact form of: “the period along the direction of  $\mathbf{k}_{\parallel}$  of an acoustic excitation whose wave vector component is  $\mathbf{k}_{\parallel}$ ”.

In the direction perpendicular to the planar external surface (the direction of depth), two types of space dependence are instead found. A set of modes takes advantage of the (semi) infiniteness of the medium, and maintains a space periodicity, conveniently represented by a wave vector  $\mathbf{k}_{\perp}$  perpendicular to the surface. These modes are thus characterized by a full three dimensional wave vector  $\mathbf{k} = \mathbf{k}_{\parallel} + \mathbf{k}_{\perp}$ , and are completely analogous to those of an infinite medium: they are the bulk waves, which are reflected at the surface. There is no upper limit to their wavelengths, and no lower limit to their frequencies. The only novelties are introduced upon reflection: firstly, in the direction perpendicular to the surface the interference between the incident and the reflected waves generates a standing wave pattern. Secondly, the mere superposition of an incident longitudinal wave and its reflected counterpart would not satisfy the stress free boundary conditions. Therefore, upon reflection, an incident longitudinal wave is partially reflected into a longitudinal wave, having the same  $\mathbf{k}_{\parallel}$  and a reversed component  $\mathbf{k}_{\perp}$ , and partially converted into a transversal wave, having the same frequency and the same  $\mathbf{k}_{\parallel}$ , but a different value of  $\mathbf{k}_{\perp}$ , because it has a different velocity [1, 3]. The dual conversion occurs for an incident transversal wave.

However, in the presence of this boundary, the elastodynamic equations admit another set of solutions, which are not periodic in the direction perpendicular to the external surface. They are the surface acoustic waves (SAWs), of which the

Rayleigh wave, the only one existing at the free surface of a semi-infinite homogeneous medium, is the prototype. The Rayleigh wave has a displacement field which decays exponentially with depth, with a decay length which is uniquely determined by the elastodynamic equations, and turns out to be very close to  $\lambda_{\parallel}$ ; it is thus confined in the neighborhood of the external surface [1, 3, 5]. The Rayleigh wave also has another character typical of the modes induced by confinement: they do not have a specific polarization. The displacement vector  $\mathbf{u}$  of the Rayleigh wave has a direction which changes with depth; it always is in the plane identified by  $\mathbf{k}_{\parallel}$  and by the normal to the surface, which is called the sagittal plane, but the two components vary with depth in different ways. The Rayleigh wave has its own velocity  $v_R$ , lower than that of any bulk wave:  $v_R < v_t < v_l$  [1, 3, 5]. Acoustic modes having similar properties can also appear at the surface separating two media in perfect adhesion.

In the semi-infinite case the medium still has no intrinsic length scale. Both periods,  $\lambda_{\parallel}$  and  $2\pi/|\mathbf{k}_{\perp}|$ , can go in continuity from infinity to the smallest meaningful values, and correspondingly the frequencies go from zero to a very high upper limit. Accordingly, the bulk waves and the Rayleigh wave are non-dispersive, also the velocity  $v_R$  being independent from  $|\mathbf{k}_{\parallel}|$ ; the dispersion relation  $\omega = v_R |\mathbf{k}_{\parallel}|$  is linear. However, for any value of  $\mathbf{k}_{\parallel}$ , the value of  $\lambda_{\parallel}$ , which determines the decay length, somehow sets a length scale. It can approximately be said that the value of  $v_R$  is mainly determined by the properties of the medium up to a depth  $\lambda_{\parallel}/2$ ; in other words, the Rayleigh wave is a probe which senses the properties of the medium up to that depth [6]. The component  $\mathbf{k}_{\perp}$  exploring the whole interval from zero to the maximum meaningful value, we have  $|\mathbf{k}| = |\mathbf{k}_{\parallel} + \mathbf{k}_{\perp}| \geq |\mathbf{k}_{\parallel}|$ , and  $\lambda$  cannot be below  $\lambda_{\parallel}$ . For that value of  $\mathbf{k}_{\parallel}$  we have bulk modes, whose frequencies go with continuity from  $v_t |\mathbf{k}_{\parallel}|$  till very high values, and, below this lower limit, the Rayleigh wave at an isolated frequency  $v_R |\mathbf{k}_{\parallel}|$ .

Instead, in media that are finite in at least one dimension, with a size  $D$ , the size of the object which supports the excitations sets a reference length scale. The relevance of confinement is determined by the ratio of the wavelength  $\lambda$  to the size  $D$ . On the high side, acoustic excitations having a ratio  $\lambda/D$  significantly larger than one are not supported: the size  $D$  sets an upper limit for wavelength. On the lower side, the excitations having a ratio  $\lambda/D \ll 1$ , down to the lower limit at which the continuum model loses significance, are affected in a negligible way by the finiteness of the medium. For these excitations, the medium is still almost invariant for translations of several wavelengths, and the modes are indistinguishable from traveling periodic waves. However, strictly speaking, they become standing waves, and the difference becomes evident for the excitations whose ratio  $\lambda/D$  is not far from unity. For these excitations, the medium is definitely not invariant for translations of few wavelengths: the modes cannot have a well-developed periodicity, and are strongly affected by confinement.

Objects having a high aspect ratio, like thin layers or beams, or nanorods, are often of interest: in one or two dimensions their size is  $D$ , in the remaining direction(s) it is  $D'$ , with  $D \ll D'$ . The consequences of confinement within  $D$  are evident for excitations having  $\lambda \sim D$ , well before the finiteness of  $D'$  becomes perceptible. These excitations can be analyzed as if in the other direction(s) the medium was still infinite: the excitations are still periodic in this (these) direction(s), characterized by a wave vector  $\mathbf{k}_{\parallel}$ . The effects of the finiteness of  $D'$  become evident only when  $\lambda_{\parallel} \sim D'$ .

Again, the Rayleigh waves paradigmatically indicate the consequences of a finite size. We can consider a slab, whose thickness is the characteristic size  $D$ , and which can be considered infinite in the other directions. Bulk waves with  $\lambda/D \ll 1$  are affected in a negligible way by the finiteness of the medium, as well as the SAWs having  $\lambda_{\parallel} \ll D$ . At such wavelengths, the Rayleigh waves are confined in the

neighborhood of the two surfaces, and do not interact with each other, while the bulk waves have a component  $k_{\perp}$  which is now discretized (the period  $2\pi/|k_{\perp}|$  must be an integer sub-multiple of  $D$ ) but with a narrow spacing. Instead, when  $\lambda$  increases and approaches  $D$ , on one side this discretization becomes relevant, and, on the other side, the tails of the displacement fields of the Rayleigh waves at the two surfaces superpose. The two SAWs then merge into modes which are typical of the slab, with displacement fields which extend throughout the thickness, their depth dependence being not periodic. Among them, the bending modes of the slab [7, 8], reminiscent of the bending modes of a membrane, which are different from the transversal bulk modes, which are shear modes, not bending modes. The dispersion relation  $\omega = \omega(|k_{\parallel}|)$  has discrete branches which correspond to these modes. They are nonlinear, i.e. dispersive, meaning that their velocities depend on the period  $\lambda_{\parallel}$ , more precisely on the ratio  $\lambda_{\parallel}/D$ , i.e. on the product  $D|k_{\parallel}|$ ; they asymptotically tend to the linear dispersion relations of the infinite medium when the product  $D|k_{\parallel}|$  becomes large.

In the case of a film supported by a substrate, which can be generalized to stratified media, the layer thickness sets the characteristic size  $D$ . Bulk waves in any layer, with  $\lambda/D \ll 1$ , and the Rayleigh wave at the surface of the outermost layer with  $\lambda_{\parallel} \ll D$ , are indistinguishable from those in a semi-infinite medium of the same material. Instead, waves with  $\lambda$ , or  $\lambda_{\parallel}$ , comparable to, or larger than  $D$  (if the substrate is semi-infinite  $\lambda$  can go to infinity) have a displacement field which extends over various layers, and have properties which depend on the properties of the various layers. In particular, the Rayleigh wave becomes a generalized Rayleigh wave, whose depth dependence is affected by the transition from the film to the substrate. When  $\lambda_{\parallel} \gg D$  the decay length is also much larger than the film thickness, and the displacement field of the generalized Rayleigh wave is mostly in the substrate. In this limiting case the generalized Rayleigh wave approaches the Rayleigh wave of the bare substrate, only slightly modified by the presence of the supported layer. Depending on the properties of the layers, namely on their acoustic velocities, other SAWs can be supported. For instance, an acoustically slow layer can act as a waveguide, confining some other modes, like the Sezawa modes. These modes are reminiscent of the modes of a slab, but instead of having stress free boundary conditions they have, on the substrate side, continuity boundary conditions, and tails of the displacement field which extend into the adjacent layers. Obviously also these modes are dispersive, their velocities depending on the product  $D|k_{\parallel}|$ , or, in the case of several layers, on the products with the various thicknesses. The dispersion relations for the various branches can be numerically computed, as functions of these products and of the elastic constants and mass densities of all the layers [9, 10].

A wide slab, of thickness  $D$ , can be cut into a stripe of width comparable to  $D$ : confinement thus occurs in two directions. More generally, it is the case of a slender cylinder, of circular or non-circular cross section, of lateral size  $D$ , which can still be treated as infinite in the third direction. The parallel wave vector  $k_{\parallel}$  remains fully meaningful, although, having exclusively the axial direction, its vectorial character becomes redundant. New modes appear, namely the torsional ones, beside the bending or flexural ones, and the dilatational ones. In the case of circular cylinders they obey the Pochhammer-Cree Equations [11, 12], in which, as it often happens in cylindrically symmetric cases, Bessel functions play a crucial role. More general cases can be analyzed by the so-called xyz algorithm [13, 14], which has been applied to rectangular [15], circular [16] and hexagonal [17] cases, and also to more complex cases like superlattices [18].

The dispersion relation  $\omega = \omega(|k_{\parallel}|)$  has a significant number of branches, which asymptotically tend to the linear dispersion relations of the infinite medium when



the product  $D|\mathbf{k}_{\parallel}|$  becomes large. For smaller values of  $D|\mathbf{k}_{\parallel}|$ , instead, these branches remain separate, and nonlinear. In particular, several branches have a non-null frequency for  $|\mathbf{k}_{\parallel}| = 0$ ; they correspond to modes, like e.g. the radial breathing modes, which can have a non-traveling character [12]. Furthermore, for small values of  $D|\mathbf{k}_{\parallel}|$ , the dispersion relations of most of these modes have a slope much smaller than the velocities  $v_t$  or  $v_l$ , meaning a low group velocity, and in some cases even a negative slope [19].

Finally, for objects whose aspect ratio is not far from unity, and therefore in which confinement is along all the three directions to a size of the same order  $D$ , the general considerations apply. Namely, all the excitations have the character of discrete standing waves. For ratios  $\lambda/D \ll 1$  the discretization has a narrow spacing, the modes are almost indistinguishable from those of an infinite medium, and can still be characterized by a wavevector  $\mathbf{k}$ , or  $\mathbf{k}_{\parallel}$ . Instead, for ratios  $\lambda/D$  not far from unity the modes, in general, do not have a regular periodicity, and any wavevector loses its meaning. The modes have clearly separate frequencies, are strongly affected by confinement, and strongly depend on the shape of the object. Note that for objects which become nanometric the regime in which  $\lambda/D \ll 1$  does not exist, because it would mean wavelengths at which the continuum model breaks down.

Two main geometries are of interest, both for fundamental studies and for technological applications. Firstly, the planar geometry of thin films, in which confinement is in only one direction, the critical size  $D$  is the thickness, the wider size  $D'$  being the lateral extension of the layer. The typical examples are the supported films and the resonators, either in the form of a clamped membrane or of a cantilever, or a bridge. Secondly, the linear geometry of beams and of nanorods, in which confinement is in two directions, the critical size  $D$  is the diameter, the wider size  $D'$  being the length. The two characteristic lengths,  $D$  and  $D'$ , identify two length ranges; acoustic excitations can be probed at the two length scales, which obviously correspond to two frequency ranges.

Ultrasonic waves of wavelength comparable to  $D$  are not affected by the finiteness of  $D'$ , or by the precise shape of the object supporting them: they see the other dimensions as infinite. The properties of the waves depend on the material properties, and the value of  $D$  determines the existence of the discrete modes, which can be observed. In some cases the properties of the waves are also affected by the value of  $D$ , as it happens for supported films when the ratio  $\lambda/D$  is close to unity: in this case the displacement field of the wave appreciably penetrates into the substrate, and is affected by its properties.

Instead, for acoustic excitations at the scale of  $D'$ , the effective stiffness for the vibrational modes depends on the material properties, but also, crucially, on the value of  $D$ . The properties of the waves thus depend on the material properties and on the value of  $D$ , while the value of  $D'$  determines the existence of the discrete modes, which can be observed. In fact the fundamental, and higher order, oscillations of a cantilever can be seen as standing flexural waves, of wavelength comparable to of  $D'$ , and of effective stiffness dependent on  $D$ .

The two ranges of wavelength identify two classes of measurements. A first class exploits purpose-built testing structures, which determine the value of  $D'$ ; they are probed at effective wavelengths of this order. Typically, their oscillations are mechanically actuated by piezoelectric means. The next section is devoted to them. A second class exploits ultrasonic waves at wavelengths comparable to  $D$ . Their excitation is achieved by short laser pulses, or simply by thermal motion. Their detection typically requires optical means, and can be performed either in the time domain or in the frequency domain.



### 3. Measurement techniques based on testing structures

As repeatedly underlined, the elastic continuum model is meaningful down to almost the molecular scale. Techniques based on acoustic excitations are therefore, in principle, applicable to objects down to the nanometric scale. Their effective application depends on the availability of appropriate transducers to excite and to detect the relevant acoustic excitations. In the case of macroscopic objects, the typical techniques are based on piezoelectric transducers, which can be exploited for both excitation and detection. Specific devices are available, and specific instruments, like acoustic microscopes. An alternative, for what concerns detection, is offered by laser Doppler vibrometry. It has the advantages of the optical techniques: light is a massless probe, contactless, which does not load the measured object, is free from own resonances, has a bandwidth that is essentially determined by electronics (the light sensor and the amplification). Furthermore, it can measure small objects, and can measure surfaces which are difficultly accessible, or on which the application of a detector is not possible, e.g. because of their temperature.

In the case of small objects, down to micrometric or sub-micrometric scale, the exploitation of a separate measurement device in mechanical contact becomes impossible. Mechanical actuation by piezoelectric means is still possible either in the case of resonators, by an external actuator which shakes the whole assembly containing the resonant structure, or by inclusion, by nanofabrication techniques, of a piezoelectric (nano)layer as an integral part of the structure being tested. MEMS/NEMS of this type can also be actuated by electrostatic means. In some cases, the test system can have a structure analogous to that of a complete device, and comprehend, beside the possibility of excitation by piezoelectric or electrostatic means, the ability of measurement, e.g. by capacitive detection or by an interdigitated transducer (IDT). Except for these cases, optical detection is mandatory. Laser Doppler vibrometry is the measurement technique of choice, if the measured system has a flat surface of sufficient size. Otherwise, interferometric techniques have been exploited.

A specific case is that of resonators: a significant effort is under way to produce high quality resonators, mainly because of their great potential for applications in sensing, signal processing, and quantum physics. The properties of a resonator can be measured in a static way, by measuring the deflection of a cantilever, or a membrane, or by measuring its resonant frequency. When a resonator is reduced to a small size, typically in the shape of a cantilever, a bridge, or a clamped membrane, its surface to volume ratio increases. Therefore phenomena, which otherwise are minor or negligible, and are not accounted for by  $q$ . (1), become non negligible; namely anelastic effects, possibly connected to internal friction phenomena, and surface phenomena, like surface tension or environmental effects [20, 21]. In particular, interaction with the environment, typically by adsorption of molecules, including water, made available by relative humidity, is the physico-chemical basis for the development of sensors. The development of high performance sensors based on nanoresonators [22, 23] is not considered here. We merely note that research in this direction has led to doubly clamped resonators of thickness down to 22 nm and aspect ratio up to 5000; the measurement of their deflection requires an interferometric technique, and their motion due to Brownian thermomechanical techniques becomes detectable [24].

However, resonant structures can be built specifically to the purpose of a precise measurement of the properties of the materials which constitute them. In order to measure the properties of tetrahedral amorphous carbon (also known as diamond-like carbon), Czaplewski et al. built, by standard techniques for the production of

MEMS, several resonators, with critical dimension down to 75 nm [25]. Excitation was in some cases electrostatic, and in other cases by shaking by an external piezoelectric actuator. Detection was, depending on the in-plane or out-of-plane deflection, by a laser deflection technique similar to that used by AFMs, or by an interferometric technique. Their results allowed them to analyze dissipation and to discuss various possible mechanisms. Exploiting flexural and torsional oscillators, and the same interferometric measurement technique, they also determined the elastic moduli as function of temperature [26]. In order to measure the properties of an assembly of only carbon nanotubes (called 'forest of nanotubes'), self-sustained only by their entwining and internal interactions, Hassan et al. built by this material cantilevers, of 1 mm length, which were electrostatically excited, and whose motion was detected by laser Doppler vibrometry [27].

The advantages of miniaturization led to explore also the sizes at which the elastic continuum approach is no longer adequate, and a Molecular Dynamics approach is more appropriate [28]. Interestingly, for membranes which become nanometric but have significantly larger lateral extension, the continuum approach remains useful, both for the theoretical analysis and the measurement technique. Membranes of nanocrystalline diamond and of piezoelectric aluminum nitride, and bilayer membranes, with thicknesses down to 220 nm and diameters up to 1 mm, have been investigated by Knoebber et al. [29] by both a static and a vibrational technique. The static technique, of more macroscopic character, was the bulge test, in which the deflection of the circular clamped membrane under gas pressure is measured; the implementation was optical, the deflection being optically measured by white light interferometry. The vibrational technique involved excitation by an external piezoelectric stack, and detection by laser Doppler vibrometry. The analysis shows that the results from the dynamical technique are less sensitive to the geometrical inaccuracies of the tested membrane. Similarly, the properties of bilayers obtained by growing nanocrystalline diamond on aluminum nitride thin films, of about 200 + 200 nm thickness, were measured producing microresonators, either cantilevers or bridges, of length up to 50  $\mu\text{m}$ , piezoelectrically actuated and measured by laser Doppler vibrometry [30]. Similar nanocrystalline diamond/aluminum nitride membranes, of thicknesses of the order of hundreds of nanometers, were still characterized by the bulge test on circular clamped membranes, of radii up to 1 mm [31].

Also in the analysis of a typical 2-D material,  $\text{MoS}_2$ , resonators have been built in the form of clamped membranes, of radii of 2 and 3  $\mu\text{m}$ , ranging from a single layer, i.e. a truly atomic thickness, up to over 90 layers. The membranes were obtained over pre-patterned circular holes in a Si substrate, and acted as 'drums'. Their motion was measured exploiting the vibrating drum membrane and the bottom of circular hole as the two mirrors of an interferometer. The continuum mechanics approach turned out to be useful in the interpretation of the experimental results, which showed the transition from the membrane regime, in which the restoring force in the oscillation is supplied by the membrane tension, to the plate regime, in which the restoring force is supplied by the bending stiffness of the plate [32].

A whole class of devices exploits the interdigitated transducers (IDTs) to launch and resonantly detect surface acoustic waves. A piezoelectric layer is a crucial component of these devices. When the lithographic techniques to produce IDTs is available, devices have been produced specifically for the aim of measuring the properties of the material which constitute them. Measurements have been performed on various forms of artificial diamond (nanocrystalline diamond, nitrogenated diamond-like carbon), of particular interest for devices exploiting surface waves and IDTs because of their high acoustic velocity [33–35].

#### 4. Measurement techniques based on ultrasonic waves

Various measurement techniques based on vibrations and acoustic waves rely on impulsive mechanical excitation of vibrational modes or of waves. Mechanical excitation by an impact has been analyzed in detail [36, 37], and standards have been issued concerning it [38]. When extending these techniques towards nanomechanics, and in particular to thin films, wave excitation by laser pulses is their natural evolution. Absorption of a laser pulse, of duration  $\tau$ , induces, by thermal expansion, a sudden expansion: a strain pulse, which propagates away at the speed  $v_l$  of longitudinal sound. The mechanism of phonon generation has been analyzed in detail [39]. The geometry of this pulse depends on the absorption length  $\zeta$  of the optical pulse, on the distance  $v_l\tau$  traveled by the strain pulse during the laser pulse, and on the lateral size of the region on which the laser beam is focused. Metals have the shortest absorption lengths, of some nanometers, and have longitudinal sound velocities of few km/s, i.e. few  $\mu\text{m}/\text{ns}$ . With optical pulses of the order of the ns, heating and thermal expansion occur until the pulse has traveled a distance of few  $\mu\text{m}$ .

In the case of a thin supported film, of thickness  $D$  of some micrometers, or even less, a ns laser pulse launches a strain pulse which is originated in the whole thickness of the film. Such a strain pulse travels parallel to the surface, and, if the film has a sufficient lateral extension, can be detected at a distance of millimeters, measuring the transit time. This is the regime of the so-called laser ultrasonics, in which the laser is focused by a cylindrical lens. A line source is therefore present in the film, which launches two SAWs traveling in opposite directions, on a surface whose lateral size  $D'$  is large. The ratio  $\lambda_{||}/D$  can be smaller than one, implying that the displacement field is essentially confined within the film, or larger, meaning that the displacement fields of the SAWs penetrate significantly into the substrate. In the latter case a typical objective of the measurement is the detection of the (small) modification of the Rayleigh wave of the bare substrate.

With optical pulses of less than the picosecond, instead, heating and thermal expansion occur only until the strain pulse has traveled a distance of the order of the nm, i.e. less than the absorption length. The pulse displacement during excitation is thus negligible, and heating, and thermal expansion, occur only in a thin surface skin, of depth  $\zeta$ , i.e. few nm. This is the regime of the so-called picosecond ultrasonics, in which the laser is focused by a spherical lens to a spot whose width is of several micrometers, i.e. orders of magnitude wider than the depth within which thermal expansion occurs. In the case of a film of thickness  $D$ , a plane wave is therefore launched: a strain pulse, of lateral extension of several  $\mu\text{m}$ , which extends over a depth of  $\zeta$ , has leading wavelength of this same order, and travels in the direction perpendicular to the surface. Except for truly nanometric films, in this case  $\lambda/D \ll 1$ , and the finiteness of  $D$  becomes relevant thanks to the reflection of the pulse when it reaches the opposite surface. If the film is supported the reflection is only partial, part of the pulse being transmitted; the echo however returns to the surface, where it can be detected, and where it is again reflected back. The transit time, of the order of the ns, or less, is measured by a pump-and-probe technique, in which a short, weaker, 'probe' pulse follows the 'pump' pulse with a variable delay, and detects the time evolution of the transient induced by the pump pulse, scanning the delay until the exhaustion of the transient itself.

The technique has also been exploited for nanostructures which do not have a planar surface extending over the several micrometers of the focused spot; nanorods are an example. In this case the geometry of the strain pulse is not the simple planar one outlined above, and is rather dictated by the specific geometry of



the illuminated object(s). The detected signal contains however relevant information, whose interpretation typically requires the modeling of the specific dynamic structure of the investigated objects.

In both the above techniques a transient is induced by a pulse which is short, i.e. strongly localized in time, and also strongly localized in space, resulting in a broadband and localized pulse, whose transit is easily detected. In a different technique a similar short pulse is exploited, which produces a transient, but illuminates a wider segment of the surface with a periodic pattern, and has therefore a narrow band. Periodicity is obtained splitting the pump laser pulse in two beams, and recombining them at the surface of the sample, forming an interference pattern. The same impulsive thermal expansion thus occurs with a periodic space modulation. The periodicity, which here is called  $\lambda_{\parallel}$  and which in the literature dealing with this technique is more often called  $\Lambda$ , is selected by the interference geometry, as well as its direction: the wavevector  $\mathbf{k}_{\parallel}$  is selected by the illumination geometry. The technique is applicable to samples having a planar surface whose lateral size  $D'$  is much larger than the periodicity  $\lambda_{\parallel}$ .

The time evolution of the reflectivity (or, possibly, of the transmittance) is measured in one point, either by a continuous measurement by a fast detector, or, more frequently, by the pump-and-probe technique. The measured signal typically has a slowly declining component, corresponding to the total energy deposited by the pulse, which eventually diffuses towards the adjacent parts of the sample, and a periodic component. The periodic component is due to the SAWs which are launched in the directions of  $\mathbf{k}_{\parallel}$  and  $-\mathbf{k}_{\parallel}$ , and which form a standing wave, eventually damped, both because the two SAWs travel away, and because of intrinsic damping mechanisms, like the thermoelastic one. By the spectral analysis of the observed signal one point of the dispersion relation  $\omega = \omega(\mathbf{k}_{\parallel})$  is obtained, hence the name of 'transient grating spectroscopy'. The full dispersion relation is obtained scanning the wavevector  $\mathbf{k}_{\parallel}$ , by adjusting the geometry of the interfering beams; at least in principle, a wide interval of  $|\mathbf{k}_{\parallel}|$  is accessible. In the case of a film of thickness  $D$ , the interval from  $\lambda_{\parallel}/D \ll 1$  to  $\lambda_{\parallel}/D \gg 1$  can sometimes be scanned. It must however be noted that this is a case in which the characteristic length  $D$  is dictated, more than by the geometry of the sample, by the geometry of the excitation, i.e. by the periodicity  $\lambda_{\parallel}$  determined by the experimental set-up. In fact, as noted above, SAWs of wavevector  $\mathbf{k}_{\parallel}$  are sensitive to the properties of the medium only up to depth of approximately  $\lambda_{\parallel}/2$ .

In all the above techniques a 'pump' laser pulse induces a transient, whose time evolution is measured, with a time resolution down to the picosecond scale. The transient grating technique deserves the 'spectroscopy' name because it relies on the successive spectral analysis of the measured time signal. Instead, the vibrational spectroscopies investigate the steady state excitation of vibrational modes, due to thermal motion. They exploit continuous, not pulsed, lasers, and detect the component of the scattered light which has undergone a frequency shift, because it was inelastically scattered by the excitations present in the sample. Obviously, inelastic scattering involves some energy exchange between the optical and the acoustic fields, but, due to the smallness of the scattering cross section, this is minor, in comparison to the thermal energy. Only in special cases, namely highly confined nanostructures, the exchange can become significant. The most widespread vibrational spectroscopies, namely Raman spectroscopy and infrared spectroscopy, are not considered here because they measure vibrational excitations of non acoustic type.

Instead, Brillouin scattering is precisely the inelastic light scattering by the vibrational excitations of the acoustic type, and Brillouin spectroscopy measures it.



In a manner analogous to that of Raman spectroscopy, the sample is illuminated by a laser beam, and the scattered light is collected; the spectral analysis singles out the minor fraction which has undergone inelastic scattering by the excitations in the sample. The scattering geometry selects an exchanged wavevector  $\mathbf{k}$ , or  $k_{\parallel}$  in the case of SAWs. Therefore, also in this technique, in the case of SAWs the experimental technique selects a periodicity  $\lambda_{\parallel}$  which essentially dictates the length scale  $D$ , and the depth over which the properties of the medium are interrogated. A Brillouin spectrum supplies a point of the dispersion relation  $\omega = \omega(\mathbf{k})$  for each of the branches which give a measurable peak. With visible light, and typical properties of solid materials, the observed frequencies, i.e. the frequency shifts of light, range from few GHz to tens of GHz, i.e. a wavenumber in the range of the  $\text{cm}^{-1}$ , to be compared with the typical frequency shifts observed in Raman spectroscopy, in the range of hundreds of  $\text{cm}^{-1}$ . Accordingly, the diffraction gratings, which are the common spectrum analysers in Raman spectroscopy, do not have a sufficient resolution, and other techniques must be employed. The tandem multipass Fabry-Perot interferometer has become the standard apparatus in Brillouin spectroscopy [40]. The small observed frequencies ( $1 \text{ cm}^{-1}$  means 30 GHz or  $1.4^\circ\text{K}$ ) make the Stokes and anti-Stokes parts of the spectra symmetric, to a difference from what happens in Raman spectroscopy.

The dispersion relations  $\omega = \omega(\mathbf{k})$  of the traveling waves, whenever a wavevector  $\mathbf{k}$  can meaningfully be identified, and the frequencies of the standing waves, can be theoretically predicted, from the simplest ones of Eqs.(2) to the more complex ones which can only be numerically computed. They are all functions of the properties of the medium (or the media involved). Therefore, whenever and however they are measured, they provide access to the properties, which can be found fitting the computed dispersion relations, or the frequencies, to the measured ones. Obviously the amount of obtainable information depends on the amount, and the quality, of the experimental evidence, and on the simpler or more sophisticated way of treating it. The obtainable information ranges from a semi-quantitative comparison for a single parameter, to a complete elastic characterization of a layer.

#### 4.1 Laser ultrasonics

The laser ultrasonics technique exploits SAWs, mainly the Rayleigh wave, possibly modified by the presence of a supported film, to measure the properties of samples having a planar surface of sufficient lateral extension. The focus often is the measurement of the properties of the supported film. Waves are launched by a laser pulse, typically of nanosecond duration; visible or near UV light is typically used, often from a  $\text{N}_2$  laser at 337 nm. As mentioned above, the laser is focused by a cylindrical lens on the surface of the sample, resulting in a sudden expansion of a line-shaped region, which launches a broadband surface wave, which propagates perpendicularly to the focusing line, with a limited divergence. The surface wave is detected by the displacement it induces perpendicularly to the surface, after a propagation path, typically of millimeters.

Detection can be done by optical interferometry [41, 42], or, in a simpler way, by piezoelectric sensing: either a piezoelectric polymer foil pressed on the sample by a blade [43–47], or a piezoceramic stripe [48]. A ready-to-use commercial apparatus is also available.

Yang et al. implemented both the optical and the piezoelectric detection. They performed a systematic comparison exploiting a 320 nm  $\text{SiO}_2$  thermal oxide layer over the pristine Si substrate. The optical detection obtains lower intensity signal but also a lower background noise, and wider bandwidth: in their implementation the bandwidth of the piezoelectric detection is limited to about 120 MHz, mainly by

the piezoelectric foil exploited for transduction, while the optical detection shows substantial signal components up to almost 300 MHz [49]. The same authors then integrated the two techniques in a single apparatus.

The recorded displacement can be frequency analyzed, yielding the dispersion relation  $v_R(\omega)$  for a frequency interval that can extend over a full frequency decade (e.g. 20 to 200 MHz). As mentioned above, fitting the computed dispersion relation to the measured one allows to derive the film properties. In the case of supported films the width of the measured frequency interval can allow to appreciate the non linearity of the velocity dependence of the frequency. If this is the case, the fit of the computed dispersion relation to the measured one allows to derive both the Young modulus and the film thickness [44, 45]. If the measurement extends over a more limited frequency interval, or if the material properties and the thickness are such that the non linearity is mainly in a frequency interval external to the measured one, an independent measurement of thickness is needed. Since the waves are detected after a propagation of the order of millimeters, the obtained properties are representative of an average of the properties over this distance.

The technique has been extensively adopted to characterize diamond-like carbon films. It has been pushed to the measurement of films having thickness down to 5 nm, deposited on a Si substrate [41]. The stretch of the observed propagation path to 20 mm allowed to measure variation of the Rayleigh wave velocity below 0.25 m/s, over a velocity of about 5000 m/s for the bare Si substrate. The small variation due to the nanometric film is thus detected. Ultra nanocrystalline diamond films of micrometric thickness were more easily characterized [47]. Also the commercially available apparatus proved to be able to measure the properties of alumina films produced by the atomic layer deposition (ALD) technique, of thickness down to about ten nanometers [50].

## 4.2 Picosecond ultrasonics

Since femtosecond laser pulses became available, the so-called ‘picosecond ultrasonics technique’ exploits them; nevertheless, it is still called ‘picosecond ultrasonics’ from the picosecond, or sub-picoseconds, pulses which were available at the time in which it was first demonstrated, by the seminal work of Thomsen et al. [51, 52] and by Wright [53, 54]. It is a technique which belongs to the wide family of the optical pump-and-probe scheme, whose performances, namely resolution, crucially depend on the short duration of pulses.. As previously outlined, two length scales contribute to determine the shape of the ultrasonic field generated by the pump pulse: the absorption length  $\zeta$  of the optical pulse, i.e. the depth within which the pulse energy is deposited, and the displacement  $v_l \tau$  of the strain field in the time interval within which the energy is deposited.

Lasers in the near infrared are typically adopted, to avoid possible spurious effects, which were attributed to electronic interband transitions [55], which might be induced at shorter wavelengths. Typical metals properties correspond to absorption lengths of nanometers; aluminum is among the metals which have the shortest absorption lengths, and well absorbs at 810 nm wavelength [56]. With the typical acoustic velocities and the typical thermal diffusivities of metals, with pulse lengths below the picosecond the fraction of the pulse energy which is not reflected is deposited before both the strain pulse and the temperature rise leave the absorption length. Therefore, the (over)simplified picture can be given, according to which at the end of the pump pulse no significant motion has occurred yet, and a significant temperature rise and dilatational strain are present within an outer skin whose thickness is of the order of the absorption length  $\zeta$ . The laser being focused on a spot whose width is of several, up to few tens, micrometers, if the outer surface of the

sample is planar the strain and the temperature fields are essentially uniform across the spot, and a plane wave is launched in direction perpendicular to the surface. The pulse is localized within a depth interval of the order of  $2\zeta$ ; it crosses the layer, is reflected (only partially if the film is not free standing), and returns to the surface, where it is detected. Further round trips can also be detectable.

Detection is performed by the probe pulse, much weaker than the pump pulse, which follows it with a variable delay, controlled by a delay line. As it is typical for pump-and-probe techniques, several details of the experimental procedure are tuned to single out the reflection of the probe beam, like different polarizations of the pump and probe beams, or frequency doubling of the probe beam, and to detect small variations of the reflectivity, like differential or interferometric detection [56]. The reflectivity is modified by the strain pulse, via the elasto-optic effect: the strain modulates the optical properties of the film, both the real part and the imaginary part of the refractive index. The measured reflectivity has a slowly varying background, due to the diffusion of the heat deposited by the laser pulse towards the depth of the sample. Superposed to this background, short modulations of the reflectivity denote the arrival of the echoes at the outer surface.

The arrival of the echo(es) at the surface is thus detected, the delay providing a measure of the velocity of the longitudinal acoustic wave, for propagation in the direction normal to the surface. Some details of the detected pulse can, at least in principle, supply further information about the film and the mismatch of properties between the film and the substrate [56]. Among them, the so-called Brillouin oscillations, which are due to the interference between the fraction of the probe pulse reflected at the outer surface, and the fraction which is reflected by the traveling strain pulse. In fact, the strain pulse, which extends over a depth interval of the order of  $2\zeta$ , is a localized modulation of the refractive index, which can reflect a fraction of the probe beam [57]. The measurement of the velocity obviously depends on the knowledge of the film thickness, often obtained by X-ray reflectivity; the uncertainty about thickness is one of the leading terms in the uncertainty to be associated to the final results.

Another factor affecting the precision of results is the resolution by which the arrival times of the pulses are detected. The modulation of the reflectivity has a finite width, which is determined by the space width of the strain pulse. In turn, this space width is determined by the absorption length  $\zeta$ . Aluminum has one of the shortest absorption lengths, at least for the 800 nm wavelength, other metals, like copper, have longer absorption lengths. In order to limit the absorption length, and thus increase the resolution of the measurement, the deposition of a thin aluminum layer (tens of nanometers) on the sample is a common practice [58]. If this interaction layer is adopted, its presence cannot be neglected in the analysis of results: the additional layer contributes to the vibrational behavior of the structure being investigated. However, operation also in semiconductors, in which the absorption length is significantly longer, has been demonstrated [59].

In several cases, for film thicknesses below  $\sim 100$  nm, resolution of single echos turns out to be difficult, or impossible [60–62]. However, by a detailed analysis of the reflectivity signal, and taking into account features like the Brillouin oscillations, it has been possible to measure Pt and Fe films of thickness down to 5 nm, deposited on Si or on borosilicate glass substrates [60], and a buried TaN layer of thickness of 20 nm [58]. Layers down to very few nanometers, stacked in a periodic Mo/Si superlattice, were also investigated, exploring different periodicities within a same total thickness. The superposition of two different signals was found. One signal corresponds at the multilayer which act as a single homogeneous effective layer. The other signal corresponds to the multilayer which acts as a Bragg reflector, and confines, in the neighborhood of the outer surface, a mode, which has been called



'localized surface mode'. This mode is sensitive to fine details of the superlattice structure, namely on the outermost layer being the one with the higher or the lower acoustic impedance (in this case Si), and on the presence of the native, nanometric, oxide layer on the Si surface. These details are consistent with the X-ray reflectivity measurements, and allowed to correctly predict the acoustic behavior [63].

The picoseconds ultrasonics technique applied to laterally homogeneous specimens measures the elastic constants involved in the propagation of plane waves traveling perpendicular to the surface: only the out-of-plane elastic characterization of the film is achieved. To overcome this limitation, non homogeneous interaction layers have been exploited, namely cut by lithographic techniques to obtain periodic structures [64–66]. It was thus possible to excite vibrational modes of different types [64]: modes of single specific structures, either nanopillars [64, 65] or nanowires [66], collective modes of these nanostructures, coupled via their substrate, and modes of the substrate layer, traveling not only in the direction perpendicular to the surface. The deposition of a metallic grating on a transparent sample allowed to diffract the pump pulse in different orders, obtaining what has been called time-domain Brillouin scattering, and measuring a whole range of acoustic frequencies in a single optical configuration [67].

The acousto-optic (or photoelastic) coupling mechanism was elucidated long ago for bulk samples and for supported films. In the case of free standing films, or membranes, it is increasingly understood that the geometric modulation of the external surfaces by the acoustic modes has a significant role. The denomination of 'moving interface effect' has been proposed [68], which can be seen as a generalization of the ripple effect, which is active at the surface of a semi-infinite medium, either homogeneous or layered.

Detailed analyses have been performed for free standing membranes [8], experimentally confirmed with non-constrained, single crystal, Si nanomembranes (thickness 260 nm), for nanoscale structures like cavities and waveguides [68], and for integrated photonic waveguides in on-chip systems [69].

With a sub-wavelength confinement, surface effects play a significant role, and the confinement induced modifications must be taken into account for both the electromagnetic and the acoustic fields. The interaction between these fields turns out to be orders of magnitude more intense than in bulky samples. In volumetric samples the laser beam is only a probe that senses the thermally excited vibrational states, while in strongly confined media the 'stimulated Brillouin scattering' is achievable, in which the electromagnetic beam excites some acoustic mode, and then interacts with it. The strong energy exchange between the trapped light and the acoustic modes, for which the name 'Brillouin optomechanics' has been proposed [70], is exploited in a whole new breed of chip based devices, which include lasers, amplifiers, filters, delay lines and isolators [70, 71]. Here, we do not address this rapidly growing 'optomechanics' field, since we are here focused on the measurement techniques, rather than the device development.

The picosecond ultrasonics technique has proven to be useful also in the measurements of nanorods. In the case of nanorods, the effects of confinement manifest themselves to a high degree. The dispersion relations of both photons and phonons are modified in the nanowires, enhancing interactions and generating peculiar phenomena like stimulated Brillouin scattering, induced transparency, 'slow light' and 'fast light' [72]. The concept of parallel wavevector  $k_{\parallel}$  remains meaningful, but can only have the fixed direction of the nanorod, meaning that scattering can only be forward, with of  $k_{\parallel} = 0$ , i.e. probing resonant phononic modes, or backward, with of  $k_{\parallel} = 2q_{\parallel}$  ( $q_{\parallel}$  being the component of the optical wavevector), probing traveling phonons. Since, furthermore, the focusing spot is wider than the nanorod, illumination is homogeneous across the nanorod.



Some experiments have been on single suspended nanowires. Copper nanorods (diameter 200 nm, length up to 5  $\mu\text{m}$ ) suspended across a lithographically obtained trench have been tested by standard techniques for picosecond ultrasonics (100 fs pulses, at the wavelength of 800 nm) [73]. The breathing modes at  $k_{\parallel} = 0$  have been detected.

However, most experiments have been performed on ‘forests’ of nanowires, either grown on particle seeds, regularly or irregularly positioned, or obtained by etching techniques. In the case of regular positions they form a photonic crystal, in which electromagnetic modes specific of single nanowires, and therefore sensitive to the nanowire diameter, can be detected, but also, depending on the period, also collective electromagnetic modes, sensitive to the photonic crystal period, can be observed. Nanorods with a diameter of the order of 100 nm, heights of several hundred nanometers, and periods ranging from few hundred nanometers to few micrometers have been produced and investigated.

One of the first observations of the vibrational modes of nanorods was obtained by the standard set up for cw Brillouin spectroscopy. Scattering was observed from monocrystalline GaN nanowires, of wurtzite structure, several micrometers long, spontaneously nucleated at the irregular surface of a GaN matrix layer over a Si substrate. Measurements were compared to a finite elements simulation; the analysis had to take into account the dispersion of the diameters, with an average value of 190 nm and a variance of 40 nm. Several branches of the dispersion relation could however be identified [74].

Successive investigations were performed by the picosecond ultrasonics technique, with focused beam spots of tens of micrometers, illuminating a high number of nanorods. GaAs nanorods were fabricated by a standard etching process from a pristine GaAs substrate, covered by a thin gold layer, such that each nanorod had at its tip a gold disk, which acted as transducer, absorbing the pump pulse and launching the acoustic pulse along the nanorod [75].

A square lattice was produced, with nanorods 720 nm long, exploring intervals of diameter (130–270 nm) and of period (300–350 nm). Square lattices of InP nanowires, grown over gold seed particles in regular pattern, with 180 nm diameter and period of 400 nm, were measured by a pump and probe technique. Measurements were compared to a detailed computation of the complicated dispersion relation [76]. This measurement allowed to validate the whole technique, which was then applied to GaAs nanorods, grown over gold seeds in an irregular pattern. Nanorods with the normal zincblende structure, as well as with the wurtzite structure, which in the bulk form is metastable, and was not previously measured, have been investigated; Diameters respectively of 100 nm and 70 nm, with lengths above 1.5  $\mu\text{m}$ . The elastic constants were derived with a resolution sufficient to appreciate the difference between the two structures [77]. Hexagonal lattices of hexagonal GaAs pillars were also produced, of diameters between 103 and 135 nm, exploring lengths up to several micrometers, and pitches from 700 nm to 3  $\mu\text{m}$  [78]. Also this measurement was accompanied by a detailed modeling, allowing to detect up to 10 branches.

The picosecond ultrasonics technique can also investigate nanoobjects, whose aspect ratio is not too far from unity, and in which confinement occurs at its maximum degree. The same concept of parallel wavevector  $k_{\parallel}$  loses its significance, only standing waves exist, whose configuration strongly depends on the geometry of the object. An extensive and detailed review of work in this area was given [79], and a more recent one focused on the measurement techniques [80]. Recent works include the analysis of compound nanoparticles [81], analyses concerning the exploitation of nanoplates as antennas in the conversion from the laser pulse to the acoustic pulse [82], and work in the direction of the imaging of acoustic modes [83].

### 4.3 Transient grating spectroscopy

The Transient grating spectroscopy (TGS) technique, which is also called Impulse Stimulated Thermal Scattering (ISTS) or Impulsive Stimulated Scattering (ISS) is an evolution of the Laser ultrasonics technique. As its 'parent' technique, it is appropriate for samples having an external planar surface of sufficient width, and is perfectly suited for the measurement of films. In the conventional laser ultrasonics technique the excitation is impulsive in time, and localized in space (the laser pulse is typically focused into a line by a cylindrical lens), resulting in a broadband pulse which is launched, and detected at some distance. The transit time is thus measured. The possibility of excitation over a more extended region, with a periodic pattern, resulting in a narrowband pulse, was considered in order to increase the efficiency in the generation of the strain pulse. A periodic pattern, of periodicity  $\lambda_{\parallel}$ , can be obtained either by two beams which interfere at the surface of the sample [84] or by a hyperbolic diffraction grating [85]. The strain field generated by the pulse is the superposition of a broad, non-oscillating feature, due to the overall heating, whose decay is governed by heat diffusion, and an oscillating feature [74, 86, 87]. The oscillating signal is due to the SAWs which are launched in opposite directions, and which form a standing wave, of periodicity  $\lambda_{\parallel}$ , which is eventually damped.

The 'pump' pulse can range from the ns to the ps; wavelengths around 500 nm are typically adopted, but both longer (1064 nm) or shorter wavelengths have been adopted. The strain transient is measured by a probe laser, either a cw laser, or a pulsed laser, in a pump-and-probe scheme. The temperature relaxation is observed by the modulation of the reflectivity of the surface. The surface corrugation due to SAWs can be detected by either the deflection of the strongly focused probe laser [87], or superposing the reflected probe beam with a reference beam, in a heterodyne amplification scheme.

A boxcar configuration has become the standard one for this technique: a volumetric diffraction grating, a 'phase mask' splits the pump pulse into diffraction orders, the +1 and -1 orders are isolated and overlapped at the sample surface, using a 4f imaging system. In this configuration the heterodyne detection is adopted, with the pump and the probe beams which share the same optics, achieving a good phase stability [88–92]. While in principle the explored periodicities  $\lambda_{\parallel}$  can vary over a very interval, practical limitations limit this interval. Firstly, the focusing spots of the lasers, which cannot be too small to avoid power densities that would damage the sample, also cannot be too wide, to avoid low power densities which would lead to too weak signals. Since the focusing spot must contain at least a certain number of interference fringes, to well define the periodicity, this set an upper limit to the accessible periodicities  $\lambda_{\parallel}$ . Lower limits are set by the velocity of the detection electronics, typically avalanche photodiodes: (shorter wavelengths mean higher frequencies) and by an intrinsic limitation: the amplitude of the surface displacement, therefore its detectability, scales as the periodicity  $\lambda_{\parallel}$ . The practical lower limit of  $\lambda_{\parallel}$  is 2–3  $\mu\text{m}$  for metals, and 5–8  $\mu\text{m}$  for ceramics [6].

The experimental techniques are undergoing further developments. Among them, further refinements of the heterodyne detection [93, 94] and a technique which allows a continuous tuning of the periodicity  $\lambda_{\parallel}$  [95]. Among recent developments, the coherent space and time control of the relative phases of the interference patterns generated by successive laser pulses, which enables the control the periodic surface deformation induced by the pump pulses, which is also monitored by time-resolved X-ray reflectivity [96], and the exploitation of femtosecond pulses of extreme ultraviolet light (12.7 nm) to obtain surface periodicities  $\lambda_{\parallel}$  of 280 nm [97]. Furthermore, the possibility of performing large area 2D maps, also dealing with surface roughness [98].

Among recent applications of the technique, the characterization of nanocrystalline diamond coatings [99], and the exploitation of the optical character of the technique to perform measurements at different temperatures [100], and in situ measurements [101]. As previously mentioned, the possibility of tuning the periodicity  $\lambda_{\parallel}$  allows to choose the depth which is probed. This is particularly useful in ion irradiation experiments: the ion implantation depth is of the order of micrometers, meaning that the irradiation modified skin is of that order; the periodicity  $\lambda_{\parallel}$  can be tuned in order to investigate precisely the depth affected by irradiation [6, 102–104].

#### 4.4 Brillouin spectroscopy

Brillouin spectroscopy investigates the inelastic scattering of light by vibrational excitations of the acoustic type [105, 106]. It is therefore in principle able to investigate both traveling waves and standing waves, from bulky samples to films and to nanorods, and the name ‘Brillouin optomechanics’ has been proposed for the interaction between the electromagnetic field and the acoustic field in nanoobjects. The ability of Brillouin spectroscopy to single out a wavevector,  $\mathbf{k}$  or  $\mathbf{k}_{\parallel}$  makes it attractive whenever a wavevector can meaningfully be considered. As a tool for the measurement of material properties, surface Brillouin scattering (Brillouin scattering by SAWs) has been extensively used to characterize supported films [107–109].

Brillouin spectroscopy is performed illuminating the sample by a focused laser beam, of wavevector  $\mathbf{q}_i$  and circular frequency  $\Omega_i$ , and collecting the light scattered along a direction  $\mathbf{q}_s$ . The spectral content of the scattered light is dominated by the light elastically scattered, at  $\Omega_i$ , but can also contain the Stokes/anti-Stokes doublets due to inelastic scattering by thermally excited vibrations of circular frequency  $\omega$ , at frequencies  $\Omega_s = \Omega_i \pm \omega$ . Since the scattering geometry selects the probed wavevectors  $\mathbf{k} = \pm(\mathbf{q}_s - \mathbf{q}_i)$ , or, in the case of SAWs,  $\mathbf{k}_{\parallel} = \pm(\mathbf{q}_s - \mathbf{q}_i)_{\parallel}$ , from each spectrum one point of the dispersion relation  $\omega = \omega(\mathbf{k})$ , or  $\omega = \omega(\mathbf{k}_{\parallel})$ , is obtained for each of the branches for which a spectral peak is measured [40, 105–108].

Scattering by bulk waves occurs by the elasto-optic effect, the modulation of the refractive index by the strain: a periodic modulation, of periodicity represented by  $\mathbf{k}$ , is a weak diffraction grating, in motion at the speed of sound. Obviously scattering by bulk waves only occurs in sufficiently transparent media, in which refraction must be taken into account: the wavevectors  $\mathbf{q}_i$  and  $\mathbf{q}_s$  are refracted into  $\mathbf{q}'_i$  and  $\mathbf{q}'_s$ , and the probed wavevector is more precisely  $\mathbf{k} = \mathbf{q}'_s - \mathbf{q}'_i$ . The refractive index  $n$  has therefore a role. Scattering by surface waves, whose strain field penetrates in an outermost layer, occurs by the same mechanism, if the medium is sufficiently transparent, and by the ripple effect: the periodic corrugation of the surface induced by the wave, which also is a weak diffraction grating. In this case the probed wavevector  $\mathbf{k}_{\parallel}$  does not depend on the refractive index, since Snell’s refraction law states that, for any optical wavevector  $\mathbf{q}$ , the component  $\mathbf{q}_{\parallel}$  parallel to the surface remains unchanged upon refraction. In metals scattering occurs only by surface waves, by the ripple effect.

The scattering process can also be described as follows. The spontaneous, chaotic, thermal motion can be thought as being three-dimensionally Fourier transformed into an incoherent superposition of harmonic waves, whose wavevectors have all the possible values. The scattering process probes the component of this decomposition which has precisely the wavevector  $\mathbf{k}$ , or  $\mathbf{k}_{\parallel}$ , selected by the scattering geometry. The exploitation of the thermal motion means that the excitation has the broadest band, but has small amplitude, implying, in many cases, time consuming measurements.



Brillouin spectroscopy has been used to characterize bulk materials, and surface Brillouin spectroscopy is particularly suited for the characterization of thin films, which are of our concern here. Although Brillouin spectroscopy can, in principle, be performed in various geometries [105, 108, 109], possibly scanning a wide interval of  $|\mathbf{k}|$ , or of  $|\mathbf{k}_{\parallel}|$ , the backscattering configuration ( $\mathbf{q}_s = -\mathbf{q}_i$ ) is, by far, the most frequently adopted. This occurs because the backscattering geometry maximizes  $|\mathbf{k}|$ , and its implementation is more practical. In backscattering the probed wavevector is  $\mathbf{k} = \pm 2\mathbf{q}'_i$ , with  $|\mathbf{q}'_i| = n|\mathbf{q}_i| = n2\pi/\lambda_{opt}$ , where  $\lambda_{opt}$  is the optical wavelength of the incident beam (remember that  $n$  is simply a scalar only when symmetry is at least cubic), or  $\mathbf{k}_{\parallel} = \pm 2(\mathbf{q}_i)_{\parallel}$ , with  $|(q_i)_{\parallel}| = |q_i| \sin \theta$ , where  $\theta$  is the incidence angle (the angle between the incident beam and the normal to the surface). The wavevector  $\mathbf{k}_{\parallel}$  does not depend on  $n$ , and depends on the incidence angle. Since incidence cannot be close to the normal (to avoid the specular reflections) nor too close to grazing one (because of the decline of the scattering cross section) the practically accessible range  $(\sin \theta)_{max}/(\sin \theta)_{min}$  seldom exceeds the value of 2.

For SAWs, the above relations give  $\lambda = \lambda_{opt}/(2n)$  and  $\lambda_{\parallel} = \lambda_{opt}/(2 \sin \theta)$ . This means that, with the often adopted  $\lambda_{opt} = 532$  nm, for supported films of thickness  $D$  of a couple of micrometers, or more, the condition  $\lambda_{\parallel} \ll D$  is easily accessible. We remember that in this case the Rayleigh wave at the surface of the film is insensitive to the substrate properties and to the precise value of thickness, and gives a direct access to the film properties. When films of this thickness are sufficiently transparent, also scattering by bulk waves is observable, the bulk waves being fully developed. Typical properties of metals, semiconductors and ceramics give, for these wavelengths, frequencies ranging from few GHz to several tens of GHz.

Brillouin spectroscopy was extensively exploited to characterize tetrahedral amorphous carbon films of thicknesses of hundreds of nanometers [110], tens of nanometers [111], down to a few nanometers [112]. In the case of thicker tetrahedral amorphous carbon films [3 micrometers] a detailed characterization was achieved by combining Brillouin spectroscopy and laser ultrasonics. The combination of the techniques gave access to a wide range of frequencies, allowing detailed determination of the elastic properties of the film [113]. Brillouin spectroscopy turned out to be a useful characterization tool also for other types of films of interest in materials science, like boron films [114] and amorphous and nanocrystalline tungsten films [115].

Since picosecond ultrasonics characterizes the out-of-plane properties by waves traveling normal to the surface, while Brillouin spectroscopy characterizes the in-plane properties by waves traveling along the surface, the two techniques have also been exploited in a combined way, achieving a more complete characterization [62, 116–118].

Brillouin spectroscopy also lends itself to the characterization of structures other than films or layers. In particular, single-walled carbon nanotubes were characterized, measuring Brillouin scattering by a free-standing film of pure, partially aligned, single-walled nanotubes, and analyzing the results in terms of continuum models [119]. The dependence of the measured spectra on the angle between the exchanged wavevector and the preferential direction of the tubes shows that the tube-tube interactions are weak: the tubes are vibrationally almost independent. The tubes are modeled as continuous membranes; taking into account that AFM images suggest that the tube segments contributing to scattering are not in the infinite tube length approximation, it was possible to derive the 2D Young modulus for the tube wall, achieving the first dynamic estimation of the stiffness of the tube wall. Scattering from carbon nanotubes was observed also in a different geometry,



with an ordered array of tubes, clamped at one end [120]. Brillouin spectroscopy also allowed one of the first observations of the vibrational modes of nanorods [74].

## 5. Conclusions

Nanotechnology, and nanodevices, identify a rapidly growing technological field. For the development of nanodevices a precise knowledge of the elastic properties of materials is of utmost importance, also because materials obtained at the nanoscale have properties which do not coincide with those of their bulk counterpart. Accordingly, a variety of techniques have been developed, which have proven able to investigate the material properties at the nanoscale. Most of these techniques rely on the interaction between optical electromagnetic fields, and mechanical acoustic fields. An overview has been given of these various techniques, offering elements for the evaluation of their appropriateness for different characterization needs.

## Acknowledgements


This work was supported by the project 'SpaceSolarShield', funded by Cariplo Foundation, Milano, Italy, project 2018-1780.

## Author details

Marco G. Beghi  
Department of Energy, Politecnico di Milano, Italy

\*Address all correspondence to: marco.beghi@polimi.it

## IntechOpen

© 2021 The Author(s). Licensee IntechOpen. This chapter is distributed under the terms of the Creative Commons Attribution License (<http://creativecommons.org/licenses/by/3.0>), which permits unrestricted use, distribution, and reproduction in any medium, provided the original work is properly cited. 

## References

- [1] Auld BA. Acoustic fields and Waves in Solids. Malabar, Florida: Robert E. Krieger Publishing Company; 1990. ISBN: 0898747821
- [2] Every AG. The Elastic Properties of Solids: Static and Dynamic Principles, In: Levy M, Bass H, Stern R, Keppens V, editors. Handbook of Elastic Properties of Solids, Liquids, and Gases; Volume I: Dynamic Methods for Measuring the Elastic Properties of Solids. New York: Academic Press; 2001. p. 3–36. ISBN: 01-244-5760-6
- [3] Kundu, T. Mechanics of elastic waves and ultrasonics non-destructive evaluation. In Kundu, T. editor. Ultrasonic and Electromagnetic NDE for Structure and Material Characterization: Engineering and Biomedical Applications. Boca Raton, FL: CRC Press; 2012. p. 1–98. ISBN: 9781439836637.
- [4] Levy M, Bass H, Stern R, Keppens V, editors. Handbook of Elastic Properties of Solids, Liquids, and Gases; Volume I: Dynamic Methods for Measuring the Elastic Properties of Solids. New York: Academic Press; 2001. ISBN: 01-244-5760-6
- [5] Farnell W, Adler EL (1972). Elastic wave propagation in thin layers. In: Mason WP, Thurston RN, editors. Physical Acoustics, Vol. 9. New York: Academic; 1972. p. 35–127.
- [6] Hofmann F, Short MP, Dennett CA. Transient grating spectroscopy: An ultrarapid, nondestructive materials evaluation technique. MRS Bulletin. 2019;44:392–402. DOI: 10.1557/mrs.2019.104.
- [7] Guyader J-L. Vibration in continuous media. Wiley; 2013. DOI: 10.1002/9780470612453.
- [8] Graczykowski B, Gueddida A, Djafari-Rouhani B, Butt H-J, Fytas G. Brillouin light scattering under one-dimensional confinement: Symmetry and interference self-canceling. Physical Review B. 2019;99:165431. DOI: 11.1103/PhysRevB.99.165431.
- [9] Brekhovskikh LM. Waves in layered media, 2nd Edition. London: Academic Press; 1980. ISBN: 0-12-130560-0.
- [10] Brekhovskikh LM, Godin O. Acoustics of Layered media I. Berlin: Springer-Verlag; 1990. DOI: 10.1007/978-3-642-52369-4.
- [11] Royer D, Dieulesaint E. Elastic waves in solids I: free and guided propagation. Advanced texts in physics. Berlin–Heidelberg: Springer, 1999. ISBN: 978-3-540-65932-7.
- [12] Garcia-Sanchez D, Déglise S, Thomas J-L, Atkinson P, Lagoin C, Perrin B. Acoustic confinement in superlattice cavities. Phys Rev A. 2016; 94:033813. DOI: 10.1103/PhysRevA.94.033813.
- [13] Visscher WM, Migliori A, T.Bell M, Reinert RA. On the normal modes of free vibration of inhomogeneous and anisotropic elastic objects. J Acoust Soc Am. 1991;90:2154–2162. DOI: 10.1121/1.401643.
- [14] Mante P-A, Belliard L, Perrin B. Acoustic phonons in nanowires probed by ultrafast pump-probe spectroscopy. Nanophotonics. 2018;7:1759–1780. DOI: 10.1515/nanoph-2018-0069.
- [15] Nishiguchi N, Ando Y, Wybourne MN. Acoustic phonon modes of rectangular quantum wires. J Phys: Condens. Matter 1997;9:5751–5764. DOI: 10.1088/0953-8984/9/27/007.
- [16] Li G, Lamberton Jr GA, Gladden JR. Acoustic modes of finite length homogeneous and layered cylindrical shells: Single and multiwall carbon

- nanotubes. *J Appl Phys.* 2008;104:033524. DOI: 10.1063/1.2965187.
- [17] Martínez-Gutiérrez D, Velasco VR. Acoustic waves of GaN nitride nanowires. *Surf Sci.* 2011;605:24–31. DOI: 10.1016/j.susc.2019.09.017.
- [18] Mizuno S, Nishiguchi N. Acoustic phonon modes and dispersion relations of nanowire superlattices. *J Phys: Condens Matter.* 2009;21:195303. DOI: 10.1088/0953-8984/21/19/195303.
- [19] Jean C, Belliard L, Becerra L, Perrin B. Backward propagating acoustic waves in single gold nanobeams. *Appl Phys Letters.* 2015;107:193103. DOI: 10.1063/1.4935351.
- [20] Finot E, Passian A, Thundat T. Measurement of mechanical properties of cantilever shaped materials. *Sensors.* 2008;8:3497–3541. DOI: 10.3390/s8053497.
- [21] Hasheminejad SM, Gheshlaghi B. Eigenfrequencies and quality factors of nanofilm resonators with dissipative surface stress effects. *Wave motion.* 2013;50:94–100. DOI: 10.1016/j.wavemoti.2012.07.001.
- [22] Chaste J, Eichler A, Moser J, Ceballos G, Rurali R, Bachtold A. A nanomechanical mass sensor with yoctogram resolution. *Nature Nanotechnol.* 2012;7:301–304. DOI: 10.1038/NNANO.2012.42.
- [23] Schmid S, Villanueva LG, Roukes ML. *Fundamentals of nanomechanical resonators.* Cham, Switzerland: Springer; 2016. DOI: 10.1007/978-3-319-28689-1.
- [24] Zhou J, Moldovan N, Stan L, Cai H, Czaplewski DA, Lopez D. Approaching the strain-free limit in ultrathin nanomechanical resonators. *Nano Letters.* 2020;20:5693–5698. DOI: 10.1021/acs.nanolett.0c01027.
- [25] Czaplewski DA, Sullivan JP, Friedmann TA, Wendt JR. Mechanical dissipation in tetrahedral amorphous carbon. *J Appl Phys.* 2005;97:023517. DOI: 10.1063/1.1821638.
- [26] Czaplewski DA, Sullivan JP, Friedmann TA, Wendt JR. Temperature dependence of the mechanical properties of tetrahedrally coordinated amorphous carbon thin films. *Applied Physics Letters.* 2005;87:161915. DOI: 10.1063/1.2108132.
- [27] Hassan MO, Nojeh A, Takahata K. A microcantilever of self-suspended carbon nanotube forest for material characterization and sensing applications. *Appl Phys Lett.* 2020;117:013101. DOI: 10.1063/5.0012533.
- [28] Vallabhaneni AK, Rhoads JF, Murthy JY, Ruan X. Observation of nonclassical scaling laws in the quality factors of cantilevered carbon nanotube resonators. *J Appl Phys.* 2011;110:034312. DOI: 10.1063/1.3611396.
- [29] Knoebber F, Zuerbig V, Heidrich N, Hees J, Sah RE, Baeumler M, Leopold S, Paetz D, Ambacher O, Lebedev V. Static and dynamic characterization of AlN and nanocrystalline diamond membranes. *Thin Solid Films.* 2014;558:267:271. DOI: 10.1016/j.tsf.2014.03.015.
- [30] Hees J, Heidrich N, Pletschen W, Sah RE, Wolfer M, Williams OA, Lebedev V L, Nebel CE, Ambacher O. Piezoelectric actuated micro-resonators based on the growth of diamond on aluminum nitride thin films. *Nanotechnology.* 2013;24:025601. DOI: 10.1088/0957-4484/24/2/025601.
- [31] Zuerbig V, Hees J, Pletschen W, Sah RE, Wolfer M, Kirste L, Heidrich N, Nebel CE, Ambacher O, Lebedev V. Elastic properties of ultrathin diamond/AlN membranes. *Thin Solid Films.* 2014;558:267:271. DOI: 10.1016/j.tsf.2014.03.015.

- [32] Castellanos-Gomez A, van Leeuwen R, Buscema M, van der Grant HSJ, Steele GA, Venstra WJ. Single-Layer MoS<sub>2</sub> Mechanical Resonators. *Advanced Materials*. 2013;25:6719–6723. DOI: 10.1002/adma.201303569.
- [33] Kim JY, Chung HJ, Kim HJ, Cho HM, Yang HK, Park JC. Surface acoustic wave propagation properties of nitrogenated diamond-like carbon films, *J of Vacuum Science and Technology A*. 2000;18:1993–1997. DOI: 10.1116/1.582460.
- [34] Bi B, Huang W-S, Asmussen J, Bolding B. Surface acoustic waves on nanocrystalline diamond. *Diamond and Related Materials*. 2002;11:677–680. DOI: 10.1016/S0925-9653(01)00621-5.
- [35] Shih W-C, Wang M-J, Nan Lin I. Characteristics of ZnO thin film surface acoustic wave devices fabricated using nanocrystalline diamond film on silicon substrate. *Diamond & Related Materials*. 2008;17:390–395. DOI: 10.1016/j.diamond.2008.01.082.
- [36] D'Evelyn MP, Taniguchi T. Elastic properties of translucent polycrystalline cubic boron nitride as characterized by the dynamic resonance method. *Diamond and Related Materials*. 1999;8:1522–1526. DOI: 10.1016/S0925-9635(99)00077-1.
- [37] Nieves FJ, Gascon F, Bayon A. Precise and direct determination of the elastic constants of a cylinder with a length equal to its diameter. *Review of Scientific Instruments*. 2000;71:2433–2439. DOI: 10.1063/1.1150632.
- [38] ASTM International. E1876–15 Standard Test Method for Dynamic Young's Modulus, Shear Modulus, and Poisson's Ratio by Impulse Excitation of Vibration. West Conshohocken, PA: ASTM International. 2011. DOI: 10.1520/E1876-15.
- [39] Ruello P, Gusev VE. Physical mechanisms of coherent acoustic phonon generation by ultrafast laser action. *Ultrasonics*. 2015;56:21–35. DOI: 10.1016/j.ultras.201406.004
- [40] Sandercock JR. Trends in Brillouin scattering: Studies of opaque materials, supported films, and central modes. In: Cardona M, Güntherodt G, editors. *Light Scattering in solids III. Topics in Applied Physics*, vol 51. Berlin: Springer; 1982. p. 173–206. DOI: 10.1007/3540115137\_6
- [41] Neubrand A, Hess P. Laser generation and detection of surface acoustic waves: Elastic properties of surface layers. *Journal of applied physics*. 1992;71:227–238. DOI: 10.1063/1.350747
- [42] Whitfield MD, Audic B, Flannery CM, Kehoe LP, Crean GM, Jackman RB. Characterization of acoustic Lamb wave propagation in polycrystalline diamond film by laser ultrasonics. *Journal of Applied Physics*. 2000;88:2984–2993. DOI: 10.1063/1.1286010
- [43] Lehmann G, Hess P, Weissmantel S, Reisse G, Scheible P, Lunk, A. Young's modulus and density of nanocrystalline cubic boron nitride films determined by dispersion of surface acoustic waves. *Applied Physics A*. 2002;74:41–45. DOI: 10.1007/s003390100897
- [44] Schneider D, Schwarz T, Scheibe H-J, Panzner M. Non destructive evaluation of diamond-like carbon films by laser induced surface acoustic waves. *Thin Solid Films*. 1997;295:107–116. DOI: 10.1016/S0040-6090(96)09163-8
- [45] Schneider D, Witke T, Schwarz T, Schoneich B, Schultrich B. Testing ultra-thin films by laser-acoustics. *Surface and Coatings Technology*. 2000;126:136–141. DOI: 10.1016/S0257-8972(99)00672-6
- [46] Coufal H, Grygier R. Broadband detection of laser-excited surface acoustic waves by a novel transducer



- p>employing ferroelectric polymers. J Acoustical Society of America. 1992;92: 2980. DOI: 10.1121/1.404363
- [47] Lee YC, Lin SJ, Buck V, Kunze R, Schmidt H, Lin CY, Fang WL, Lin IN. Surface acoustic wave properties of natural smooth ultra-nanocrystalline diamond characterized by laser-induced SAW pulse technique. *Diamond & Related Materials*. 2008;17:446–450. DOI: 10.1016/j.diamond.2007.08.25
- [48] Webersen M, Johannesmann S, Duechting J, Claes L, Henning B. Guided ultrasonic waves for determining effective orthotropic material parameters of continuous fiber reinforced thermoplastic plates. *Ultrasonics*. 2018;84:53–62. DOI: 10.1016/j.ultras.2017.10.005
- [49] Yang F, Dorantes-Gonzalez DJ, Chen K, Lu Z, Jin B, Li Y, Chen Z, Hu X. An integrated laser-induced piezoelectric/differential confocal surface acoustic wave system for measurement of thin film Young modulus. *Sensors*. 2012;12:12208–12219. DOI: 10.3390/s120912208
- [50] Zhang Q, Xiao X, Cheng Y-T, Verbrugge MW. A non destructive method for measuring the mechanical properties of ultrathin films prepared by atomic layer deposition. *Applied Physics Letters*. 2014;105:061901. DOI: 10.1063/1.4892539
- [51] Thomsen C, Strait J, Vardeny Z, Maris HJ, Tauc J, Hauser JJ. Coherent phonon generation and detection by picoseconds light pulses. *Physical Review Letters*. 1984;53:989–992. DOI: 10.1103/PhysRevLett.53.989
- [52] Thomsen C, Grahn HT, Maris HJ, Tauc J. Surface generation and detection of phonons by picoseconds light pulses. *Physical Review B*. 1986;34:4129–4138. DOI: 10.1103/PhysRevB.34.4129
- [53] Wright OB, Kawashima K. Coherent phonon detection from ultrafast surface vibrations. *Phys. Rev. Letters*. 1992;69: 1668–1671. DOI: 10.1103/PhysRevLett.69.1668.
- [54] Wright OB. Thickness and sound velocity measurement in thin transparent films with laser picosecond acoustics. *J. Appl. Phys.* 1992;71:1617–1629. DOI: 10.1063/1.351218.
- [55] Devos A, Côte R. Strong oscillations detected by picoseconds ultrasonics in silicon: evidence for an electronic structure effect. *Physical Review B*. 2004;70:125208. DOI: 10.1103/PhysRevB.70.125208
- [56] Vollmann J, Profunser DM, Dual J. Sensitivity improvement of a pump-probe set-up for thin film and microstructure metrology. *Ultrasonics*. 2002;40:757–763. DOI: 10.1016/S0041-624X(02)00207-X
- [57] Yu K, Devkota T, Beane G, Wang GP, Hartland GV. Brillouin oscillations from single Au nanoplate opto-acoustic transducers. *ACS Nano*. 2017;11:8064–8071. DOI: 10.1021/acsnano.7b2703
- [58] Bryner J, Profunser DM, Vollmann J, Mueller E, Dual J. Characterization of Ta and TaN diffusion barriers beneath Cu layers using picosecond ultrasonics. *Ultrasonics*. 2006;44:e1269-e1275. DOI: 10.1016/j.ultras.2006.05097
- [59] Babilotte P, Ruello P, Mounier D, Pezeril T, Vaudel G, Edely M, Breteau J-M, Gusev V. Femtosecond laser generation and detection of high-frequency acoustic phonons in GaAs semiconductors. *Physical Review B*. 2010;81:245207. DOI: 10.1103/PhysRevB.81.245207
- [60] Ogi H, Fujii M, Nakamura N, Shagawa T, Hirao M. (2007). Resonance acoustic-phonon spectroscopy for studying elasticity of ultrathin films. *Applied Physics Letters*. 2007;90: 191906. DOI: 10.1063/1.2737819

- [61] Daly BC, Bailey ST, Sooryakumar R, King SW. Noncontact optical metrologies for Young's modulus measurements of nanoporous low-k dielectric thin films. *Journal of Nanophotonics*. 2013;7:073094. DOI: 10.1117/1.JNP:7.07394
- [62] Faëse F, Poinot Cherroret D, Chatel S, Becerra L, Challali F, Djemia P, Belliard L. Mechanical properties of elementary layers involved in a multilayer optical stack by photon-acoustic phonon interaction approaches, *J. Appl. Phys.* 2018;124:125307. DOI: 10.1063/1.5030749
- [63] Belliard L, Huynh A, Perrin B, Michel A, Abadias G, Jaouen, C. Elastic properties and phonon generation in Mo/Si superlattices. *Physical Review B*. 2009;80:155424. DOI: 10.1103/PhysRevB.80.155424.
- [64] Bienville T, Robillard JF, Belliard L, Roch\_Jeune I, Devos A, Perrin B. (2006). Individual and collective vibrational modes of nanostructures studied by picosecond ultrasonics. *Ultrasonics*. 2006;44:e1289-e1294. DOI: 10.1016/j.ultras.2006.05.179
- [65] Mante PA, Robillard JF, Devos A. Complete thin film mechanical characterization using picoseconds ultrasonics and nanostructured transducers: experimental demonstration on SiO<sub>2</sub>. *Applied Physics Letters*. 2008;93:071909. DOI: 10.1063/1.2975171
- [66] Bjornsson MM, Connolly AB, Mahat S, Rachmilowitz BE, Daly BC, Antonelli GA, Myers A, Singh KJ, Yoo HJ, King SW. Picosecond ultrasonic study of surface acoustic waves on titanium nitride nanostructures. *J. Appl. Phys.* 2015;117:095305. DOI: 10.1063/1.4914048
- [67] Matsuda O, Pezeril T, Chaban I, Fujita K, Gusev V. Time-domain Brillouin scattering assisted by diffraction gratings. *Physical Review B*. 2018;97:064301. DOI: 10.1103/PhysRevB.97.064301
- [68] Pennec Y, Laude V, Papanikolaou N, Djafari-Rouhani B, Oudich M, El Jallal S, Beugnot JC, Escalante JM, Martínez A. Modeling light-sound interaction in nanoscale cavities and waveguides. *Nanophotonics*. 2014;3: 413–440. DOI: 10.1515/nanoph-2014-0004
- [69] Wolff C, Steel MJ, Eggleton BJ, Poulton CG. Stimulated Brillouin scattering in integrated photonic waveguides: Forces, scattering mechanisms, and coupled-mode analysis. *Physical Review A*. 2015;92: 013836. DOI: 10.1103/PhysRevA.92.013836
- [70] Wiederhecker GS, Dainese P, Mayer Alegre TP. Brillouin optomechanics in nanophotonic structures. *APL Photonics*. 2019;4:071101. DOI: 10.1063/1.5088169
- [71] Eggleton\_BJ, Poulton CG, Rakich PT, Steel MJ, Bahl G. Brillouin integrated photonics. *Nature Photonics*. 2019;13:664–677. DOI: 10.1038/s41566-019-0498-z
- [72] Kim\_JH, Kuzyk MC, Han K, Wang H, Bahl G. Non-reciprocal Brillouin scattering induced transparency. *Nature Physics*. 2015;11:275–280. DOI: 10.1038/NPHYS3236
- [73] Jean CJ, Belliard L, Cornelius TW, Thomas O, Toimil-Molares ME, Cassinelli M, Becerra L, Perrin B. Direct observation of Gigahertz coherent guided acoustic phonons in free-standing single copper nanowires. *J. Phys. Chem. Lett.* 2014;5:4100–4104. DOI: 10.1021/jz502170j
- [74] Johnson WL, Kim SA, Geiss R, Flannery CM, Bertness KA, Heyliger PR. Vibrational modes of GaN nanowires in the Gigahertz range. *Nanotechnology*

2012;23:495709. .DOI: 10.1088/0957-4484/23/49/495709

[75] Yang S-C, Wu Y-C, Mante P-A, Chen C-C, Chen H-P, Chou H-Y, Shih M-H, Sun C-K. Efficient excitation of guided acoustic waves in semiconductor nanorods through external metallic acoustic transducer. *Appl. Phys. Letters*. 2014;105:243101. DOI: 10.1063/1.4904414

[76] Mante P-A, Anttu N, Zhang W, Wallentin J, Chen I-J, Lehmann S, Heurlin M, Borgström MT, Pistol M-E, Yartsev A. Confinement effects on Brillouin scattering in semiconductor nanowire photonic crystal. *Physical Review B*. 2016;94:024115. DOI: 10.1103/PhysRevB.94.024115

[77] Mante P-A, Lehmann S, Anttu N, Dick KA, Yartsev A. Nondestructive complete mechanical characterization of zinc blende and wurtzite GaAs nanowires using time-resolved pump-probe spectroscopy. *NanoLetters*. 2016; 16:4792–4798. DOI: 10.1021/acs.nanolett.6b00786

[78] Kargar F, Debnath B, Kakko J-P, Säynätjoki A, Lipsanen H, NikaDL, Lake RK, Balandin AA. Direct observation of confined acoustic phonon polarization branches in free-standing semiconductor nanowires. *Nature Communications*. 2016;7:13400. DOI: 10.1038/ncomms13400

[79] Crut A, Maioli P, Del Fatti N, Vallée F. Acoustic vibrations of metal nano-objects: Time-domain investigations. *Physics Reports*. 2015;549:1–43. DOI: 10.1016/j.physrep.2014.09.004

[80] Balogun\_IEEE19] Balogun O. Optically Detecting Acoustic Oscillations at the Nanoscale Exploring techniques suitable for studying elastic wave propagation. *IEEE Nanotechnology Magazine*. 2019;13:39–54. DOI: 10.1109/MNANO.2019.2905021

[81] Zhao X, Nie Z, Feng Y, Zhao W., Zhang J, Zhang W, Maioli P, Loh Z-H. TI Ultrafast acoustic vibrations of Au-Ag nanoparticles with varying elongated structures. *Phys. Chem. Chem. Phys*. 2020;22:22728–22735. DOI: 10.1039/d0cp03260c.

[82] Devkota T, Yu K, Hartland GV. Mass loading effects in the acoustic vibrations of gold nanoplates. *Nanoscale*. 2019;11:16208–16213. DOI: 10.1039/c9nr05940g

[83] Guillet Y, Abbas A, Ravaine S, Audoin B. Ultrafast microscopy of the vibrational landscape of a single nanoparticle. *Applied Physics Letters*. 2019;114: 091904. DOI: 10.1063/1.5085157

[84] Nelson KA, Dwayne Miller RJ, Lutz DR, Fayer MD. Optical generation of tunable ultrasonic waves. *J. Appl. Phys*. 1982;53:1144–1149. DOI: 10.1063/1.329864

[85] Huang J, Krishnaswamy S, Achenbach JD. Laser-generation of narrow-band surface waves. In: *Proceedings of the IEEE 1991 Ultrasonics Symposium*; 1991; Orlando, FL, USA. New York: IEEE; 1991. vol.1, p. 537–541. DOI: 10.1109/ULTSYM.1991.234221.

[86] Fizez J. The determination of the elastic constants of isotropic solids by means of transient thermal surface gratings. *J. Applied Physics*. 2016;119: 015301. DOI: 10.1063/1.4939208

[87] Kading OW, Skurk H, Maznev AA, Matthias E., Transient thermal gratings at surfaces for thermal characterization of bulk materials and thin films. *Applied Physics A*. 1995;61:253–261. DOI: 10.1007/BF015381980

[88] Rogers JA, Fuchs M, Banet MJ, Hanselman JB, Logan R, Nelson KA. Optical system for rapid materials characterization with the transient grating technique: Application to



nondestructive evaluation of thin films used in microelectronics. *Applied Physics Letters*. 1997;71:225. DOI: 10.1063/1.119506.

[89] Maznev AA, Nelson KA, Rogers JA. Optical heterodyne detection of laser-induced gratings. *Opt. Letters*. 1998;23:1319–21. DOI: 10.1364/OL.23.001319

[90] Rogers JA, Maznev AA, Banet MJ, Nelson KA. Optical generation and characterization of acoustic waves in thin films: fundamentals and applications. *Annu. Rev. Mater. Sci.* 2000;30:117–57. DOI: 10.1146/annurev.matsci.30.1.117

[91] Landa M, Verstraeten B, Sermeus J, Salenbien R, Sedlak P, Seiner H, Glorieux C. Thermomechanical properties of single crystals evaluated by impulsive stimulated thermal scattering technique. *Journal of Physics: Conference Series*. 2011;278:012023. DOI: 10.1088/1742-6596/278/1/012023.

[92] Verstraeten B, Sermeus J, Salenbien R, Fizez J, Shkerdin G, Glorieux C. Determination of thermoelastic material properties by differential heterodyne detection of impulsive stimulated thermal scattering. *Photoacoustics*. 2015;3:64–77. DOI: 10.1016/j.pacs.2015.05.001

[93] Dennett CA, Short MP. Time-resolved, dual heterodyne phase collection transient grating spectroscopy. *Appl. Phys. Letters*. 2017;110:211106 DOI: 10.1063/1.4983716.

[94] Dennett CA, Short MP. Thermal diffusivity determination using heterodyne phase insensitive transient grating spectroscopy. *Journal of Applied Physics*. 2018;123:215109 DOI: 10.1063/1.5026429

[95] Vega-Flick A, Eliason JK, Maznev AA, Khanolkar A, Abi Ghanem M, Boechler N, Alvarado-Gil JJ, Nelson KA. Laser-induced transient grating setup

with continuously tunable period. *Rev. Sci. Instrum.* 2015;86:123101 DOI: 10.1063/1.4936767

[96] Pudell JE, Sander M, Bauer R, Bargheer M, Herzog M, Gaal P. Full spatiotemporal control of laser-excited periodic surface deformations. *Physical Review Applied*. 2019;12:024036. DOI: 10.1103/PhysRevApplied.12.024036

[97] Maznev AA, Bencivenga F, Cannizzo A, Capotondi F, Cucini R, Duncan RA, Feurer T, Frazer TD, Foglia L, Frey H-M, Kapteyn H, Knobloch J, Knopp G, Masciovecchio C, Mincigrucci R, Monaco G, Murnane M, Nikolov I, Pedersoli E, Simoncig A, Vega-Flick A, Nelson KA. Generation of coherent phonons by coherent extreme ultraviolet radiation in a transient grating experiment. *Applied Physics Letters*. 2018;113:221905. DOI: 10.1063/1.5048023.

[98] Reza A, Dennett CA, Short MP, Waite J, Zayachuk Y, Magazzeni CM, Hills S, Hofmann F. Non-contact, non-destructive mapping of thermal diffusivity and surface acoustic wave speed using transient grating spectroscopy. *Rev. Sci. Instrum.* 2020; 91:054902 DOI: 10.1063/5.0003742.

[99] Sermeus J, Verstraeten B, Salenbien R, Pobedinskas P, Haenen K, Glorieux C. Determination of elastic and thermal properties of a thin nanocrystalline diamond coating using all-optical methods. *Thin Solid Films*. 2015;590: 284–292. DOI: 10.1016/j.tsf.2015.08.007.

[100] Heczko O, Seiner H, Stoklasova P, Sedlak P, Sermeus J, Glorieux C, Backen A, Fahler S, Landa M. Temperature dependence of elastic properties in austenite and martensite of Ni-Mn-Ga epitaxial films. *Acta Materialia*. 2018; 145:298–305. DOI: 10.1016/j.actamat.2017.12.011.

[101] Grabec T, SedláčP, Stoklasová P, Thomasová M, Shilo D, Kabla M, Seiner

- H, Michal Landa M. In situ characterization of local elastic properties of thin shape memory films by surface acoustic waves. *Smart Mater. Struct.* 2016;25:127002. DOI: 10.1088/0964-1726/25/12/127002
- [102] Hofmann F, Mason DR, Eliason JK, Maznev AA, Nelson KA, Dudarev SL. Non-contact measurement of thermal diffusivity in ion-implanted nuclear materials. *Scientific Reports*. 2015;5:16042. DOI: 10.1038/srep16042
- [103] Dennett CA, So KP, Kushima A, Buller DL, Hattar K, Short MP. Detecting self-ion irradiation-induced void swelling in pure copper using transient grating spectroscopy. *Acta Materialia*. 2018;145:496–503. DOI: 10.1016/j.actamat.2017.12.007
- [104] Reza A, Zayachuk Y, Yu HB, Hofmann F. Transient grating spectroscopy of thermal diffusivity degradation in deuterium implanted tungsten. *Scripta Materialia*. 2020;174:6–10. DOI: 10.1016/j.scriptamat.2019.08.01
- [105] Grimsditch M. Brillouin scattering. In: Levy M, Bass H, Stern R, Keppens V, editors. *Handbook of Elastic Properties of Solids, Liquids, and Gases; Volume I: Dynamic Methods for Measuring the Elastic Properties of Solids*. New York: Academic Press; 2001. p. 331–347. ISBN: 01-244-5760-6.
- [106] Comins JD. Surface Brillouin scattering. In: Levy M, Bass H, Stern R, Keppens V, editors. *Handbook of Elastic Properties of Solids, Liquids, and Gases; Volume I: Dynamic Methods for Measuring the Elastic Properties of Solids*. New York: Academic Press; 2001. p. 349–378. ISBN: 01-244-5760-6.
- [107] Every AG. Measurement of the near surface elastic properties of solids and thin supported films. *Measurement Science and Technology*. 2002;13:R21-R39. DOI: 10.1088/0957-0233/13/5/201
- [108] Beghi MG, Every AG, Prakapenka V, Zinin PV. Measurement of the Elastic Properties of Solids by Brillouin Spectroscopy. In Kundu T, editor. *Ultrasonic and Electromagnetic NDE for Structure and Material Characterization: Engineering and Biomedical Applications*. Boca Raton, FL: CRC Press; 2012. p. 539–610. ISBN: 9781439836637
- [109] Beghi MG, Di Fonzo F, Pietralunga S, Ubaldi C, Bottani CE. Precision and accuracy in film stiffness measurement by Brillouin spectroscopy. *Review of Scientific Instruments*. 2011;82:053107. DOI: 10.1063/1.3585980
- [110] Chirita M, Sooryakumar R, Xia H, Monteiro OR, Brown IG. Observation of guided longitudinal acoustic modes in hard supported layers. *Physical Review B*. 1999;60:R5153-R5156. DOI: 10.1103/PhysRevB.60.R5153
- [111] Ferrari AC, Robertson J, Beghi MG, Bottani CE, Ferulano R, Pastorelli R. Elastic constants of tetrahedral amorphous carbon films by surface Brillouin scattering. *Applied Physics Letters*. 1999;75:1893–1895. DOI: 10.1063/1.124863
- [112] Beghi MG, Ferrari AC, Teo KBK, Robertson J, Bottani CE, Libassi A, Tanner BK. Bonding and mechanical properties of ultrathin diamond-like carbon films. *Applied Physics Letters*. 2002;81:3804–3806. DOI: 10.1063/1.1510179
- [113] Berezina S, Zinin PV, Schneider D, Fei D, Rebinsky DA. Combining Brillouin spectroscopy and laser-SAW technique for elastic property characterization of thick DLC films. *Ultrasonics*. 2004;43:87–93. DOI: 10.1016/j.ultras.2004.03.006
- [114] Dellasega D, Russo V, Pezzoli A, Conti C, Lecis N, Besozzi E, Beghi M, Bottani CE, Passoni M. Boron films produced by high energy Pulsed Laser

Deposition. Materials and Design. 2017;  
134:35–43. DOI: 10.1016/j.  
matdes.2017.08.025

[115] Besozzi E, Dellasega D, Russo V,  
Conti C, Passoni M, Beghi MG.  
Thermomechanical properties of  
amorphous metallic tungsten-oxygen  
and tungsten-oxide coatings. Materials  
and Design. 2019;165:107565. DOI:  
10.1016/j.matdes.2018.107565

[116] Rossignol C, Perrin B, Bonello B,  
Djemia P, Moch P, Hurdequint H.  
Elastic properties of ultrathin  
permalloy/alumina multilayer films  
using picosecond ultrasonics and  
Brillouin light scattering. Physical  
Review B. 2004;70:094102. DOI:  
10.1103/PhysRevB.70.094102

[117] Alonso-Redondo E, Belliard L,  
Rolle K, Graczykowski B, Tremel W,  
Djafari-Rouhani B, Fytas G. Robustness  
of elastic properties in polymer  
nanocomposite films examined over the  
full volume fraction range. Scientific  
Reports. 2018;8:16986. DOI:10.1038/  
s41598-018-35335-1

[118] Abadias G, Colin JJ, Tingaud D,  
Djemia Ph, Belliard L, Tromas C. Elastic  
properties of  $\alpha$ - and  $\beta$ -tantalum thin  
films. Thin Solid Films. 2019;688:  
137403. DOI: 10.1016/j.tsf.2019.06.053

[119] Bottani CE, Li Bassi A, Beghi MG,  
Podesta A, Milani P, Zakhidov A,  
Baughman R, Walters DA, Smalley RE.  
Dynamic light scattering from acoustic  
modes in single-walled carbon  
nanotubes. Physical. Review B. 2003;67:  
155407. DOI: 10.1103/  
PhysRevB.67.155407

[120] Polomska AM, Young CK,  
Andrews GT, Clouter MJ, Yin A, Xu JM.  
Inelastic laser light scattering study of  
an ordered array of carbon nanotubes.  
Applied Physics Letters. 2007;90:  
201918. DOI: 10.1063/1.2741145